

TRANSVERSE DEFLECTING STRUCTURES FOR BUNCH LENGTH AND SLICE EMITTANCE MEASUREMENTS ON SwissFEL

P. Craievich, R. Ischebeck, F. Loehl, G.L. Orlandi, E. Prat, PSI, Villigen, Switzerland

Abstract

The SwissFEL project, under development at the Paul Scherrer Institut, will produce FEL radiation in a wavelength range from 0.1 nm to 7 nm. The facility consists of an S-band RF-gun and booster, and a C-band main linac which accelerates the beam up to 5.8 GeV. Two magnetic chicanes will compress the beam between 2 fs rms and 25 fs rms depending on the operation mode. The bunch length and slice parameters will be measured after the first bunch compressor (330 MeV) by using an S-band transverse deflecting structure (TDS). A C-band TDS will be employed to measure the longitudinal parameters of the beam just upstream of the undulator beam line (5.8 GeV). With the designed transverse beam optics, an integrated deflecting voltage of 70 MV is required in order to achieve a longitudinal resolution on a femtosecond scale. In this paper we present the TDS measurement systems to be used at SwissFEL, with a particular emphasis on the new C-band device, including hardware, lattice layout and beam optics.

INTRODUCTION

Complete characterization of the beam phase space by means of measurements of the bunch length and of the transverse slice emittance are important tasks for commissioning and optimization of SwissFEL [1]. A Transverse Deflecting Structure (TDS), such as an iris loaded wave guide or multi cell standing wave structures, is a powerful tool to reach this aim. Two TDS measurements systems will be positioned at two points in the linac: the first one (TDS-1) at 330 MeV (low energy region), after the first bunch compressor (BC1), the second (TDS-2) at the linac end (high energy region), before the upstream of the undulators. Figure 1 shows the layout of the BC1 and injector diagnostic sections where the TDS-1 is indicated. The TDS-1 will operate in a vertical streaking mode to allow measurements of the horizontal slice emittance and bunch length. This will allow the efficiency of the first compression to be estimated. Beam slice emittance will be investigated by a multi-quadrupole scan technique combined with the TDS. By means of the TDS, the beam is vertically streaked and a multi-quadrupole scan is performed only in the horizontal direction, with the constraint of keeping the vertical beam size constant over the whole scan. For this purpose five quadrupoles are foreseen to be placed downstream of the TDS. Reconstruction of the longitudinal phase space will be performed by means of the spectrometer line.

The second measurement system based on TDS is foreseen at the linac-end and with a beam mean energy between 2.1 and 5.8 GeV. Figure 2 shows the layout of the linac-end, Aramis energy collimator and diagnostic section and,

as in the injector diagnostic section, electron beam will be vertically streaked and a multi-quadrupole scan will be performed in order to measure the slice emittance. The longitudinal phase space will be measured in the Aramis collimator before the undulator line. Two standard operational modes are foreseen for the SwissFEL at 200 pC and 10 pC for the long and short pulse options, respectively. Tables 1 and 2 contain the beam and optical parameters for both long and short pulse options that have been used for the calculations in the following sections.

Table 1: Beam and optical parameters involved in the streaking process at TDS-1 diagnostic sections for both pulse length options.

Parameter	Sy.	Long	Short	Unit
Beam energy	E	330	330	MeV
$\beta@TDS$	β_d	30	30	m
$\beta@screen$	β_s	~ 5	~ 5	m
Bunch length	σ_t	290	220	fs
Emittance	$\gamma\epsilon_y$	0.30	0.11	μrad

Table 2: Beam and optical parameters involved in the streaking process at TDS-2 diagnostic sections for both pulse length options. HR is high resolution option.

Parameter	Sy.	Long	Short	HR	Unit
Beam energy	E	5.8	5.8	2.1	GeV
$\beta@TDS$	β_d	30	30	70	m
$\beta@screen$	β_s	~ 25	~ 25	~ 5	m
Bunch length	σ_t	25	2	2	fs
Emittance	$\gamma\epsilon_y$	0.43	0.18	0.18	μrad

The measurement of the transverse slice emittance requires short portions of the bunch length to be resolved at the screen after the bunch is streaked. In general, the TDS measurement strategy at SwissFEL consists in resolving the beam profile with at least 10 slices. As this will be non-critical for TDS-1, most of the TDS-2 measurements will also be achieved with the nominal beta function at the TDS and the nominal operational beam energy of SwissFEL. However, towards the shortest bunch lengths, the maximum deflecting voltage of actual deflecting structures imposes limitations on the achievable resolution. The most challenging case is the short pulse operational mode with beam energy of 5.8 GeV and a nominal rms bunch length of 2 fs. This value corresponds to the TDS-2 resolution limit with nominal beam parameters. In order to provide a reasonable "sliced beam parameter measurement" in

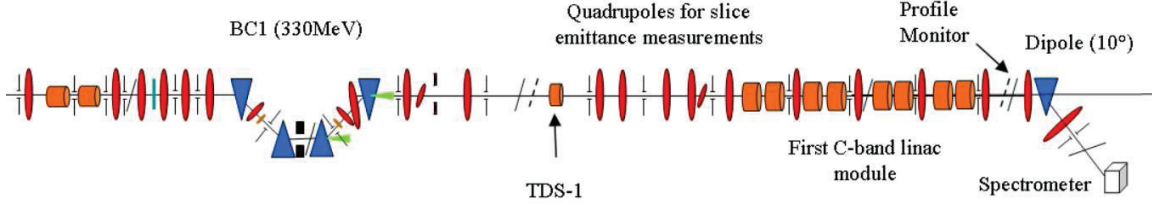


Figure 1: Layout of the BC1 and injector diagnostic sections.

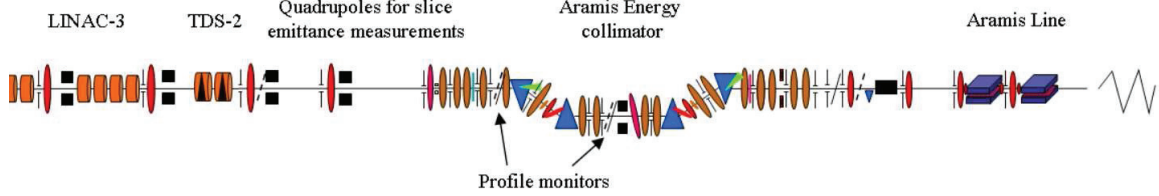


Figure 2: Layout of the linac-end including the Aramis energy collimator and the diagnostic section.

this most challenging case, the beam energy needs to be reduced to 2.1 GeV and the beta function at the TDS will be increased to 70 m. Both modifications from the nominal SwissFEL user operation mode, increases the TDS-2 time resolution.

BASIC

The well-known formulas contained in [2] concerning the dynamics of the bunch deflection as a function of the TDS parameters and of the optical Twiss parameters are used here. Perturbations to the ideal case due to the finite transverse emittance are also considered. Then, some of the basic formulae have been manipulated in order to evaluate the measurement resolution, which depends on the transverse finite emittance and on the screen resolution. The calibration factor can be written as:

$$S = \frac{\sigma_y}{\sigma_t} = \frac{eV_{\perp}}{pc} ck_{rf} \sqrt{\beta_d \beta_s} \sin \Delta\psi \quad (1)$$

where σ_y is the rms beam size of the streaked beam at the screen location and σ_z is the temporal bunch length. V_{\perp} is the integrated deflecting voltage, p the longitudinal momentum of the beam, k_{rf} the wave number, β_d and β_s are the vertical beta functions at the TDS and the screen locations, respectively, and $\sin \Delta\psi$ is the vertical betatron phase advance from the TDS to the screen. Using eq. 1 the time resolution of the measurement can be defined as:

$$\sigma_{t,R} \geq \frac{\sigma_{y0}}{S} = \sqrt{\frac{\varepsilon_{N,y}}{\gamma}} \frac{pc}{\gamma \beta_d eV_{\perp} ck_{rf} \sin \Delta\psi} \quad (2)$$

where $\varepsilon_{N,y}$ is the normalized beam vertical emittance, γ is the Lorentz factor and σ_{y0} the natural transverse beam size. A TDS induces an energy spread that may not be negligible. In order to have an estimation of the rms induced energy spread the following formula is used [3]:

$$\sigma_{\Delta E} \geq \frac{mc^2 \varepsilon_{N,y}}{\sin \Delta\psi c \sigma_{t,R}} \quad (3)$$

LOW ENERGY TDS-1

TDS at low energy will work at a maximum beam energy of 330 MeV and with an S-band RF frequency of 2998.8 MHz (the operating frequency of the injector). The deflector is a Standing Wave (SW) structure composed of 5-cells operating on the π -mode and its design is based on a deflecting structure developed for the SPARC project [4] and scaled to the SwissFEL injector operating frequency. Actually it is routinely used in the SwissFEL Injector Test Facility (SITF) [5] as a diagnostic tool. The main RF parameters of the deflector are the quality factor $Q=15600$, the transverse shunt impedance $R_{\perp} = V_{\perp}/(2P_{rf}) = 2.5M\Omega$ and the filling factor $t_f = 0.8\mu s$. Figure 3 shows calibration factor, the time resolution and induced energy spread as a function of the integrated deflecting voltage for short and long pulse options. Time resolutions are approximately 14 fs rms and 8 fs rms for the long and short pulse options, respectively. Such time resolutions permit one to resolve the beam profile with more than 20 slices for both pulse options. The induced energy spread from the TDS-1 is below 40 keV in the worse case and it is on the order of magnitude of the spectrometer resolution in the injector diagnostic section. In order to verify the time resolution and calibration factor, some measurements on the SITF have been performed. Figure 4 shows a comparison between measured and analytical calibration factor and time resolution as a function of the integrated deflecting voltage. We obtain a good agreement between model and experimental data and rms time resolution is approximately 12.4 fs at 5 MV.

HIGH ENERGY TDS-2

In order to achieve a longitudinal resolution on a femtosecond scale we have investigated some actual solutions at higher operational RF frequency since a stronger streaking of the beam improves the temporal resolution as well. In fact from S-band to X-band the wave number k_{rf} is

ISBN 978-3-95450-126-7

Table 3: RF parameters for the C-band and X-band TDS developed for SACLA[6], LCLS [7, 8] and Radiabeam technologies [9]. All structures are constant impedance and backward traveling wave structures.

Parameter	Symbol	SACLA	LCLS	Radiabeam	Unit
RF frequency	f	5.712	11.424	11.424	GHz
Length	L	1.706	1	0.46	m
Power-to-voltage	$V/L/P^{0.5}$	4	5.4	7.3	$MV/m/MW^{0.5}$
Wave number	k_{rf}	120	240	240	m^{-1}
rf input power	P	40	40	40	MW
Number of structures		2	2	4	
Integrated def. voltage	V_{\perp}	60	48	42	MV

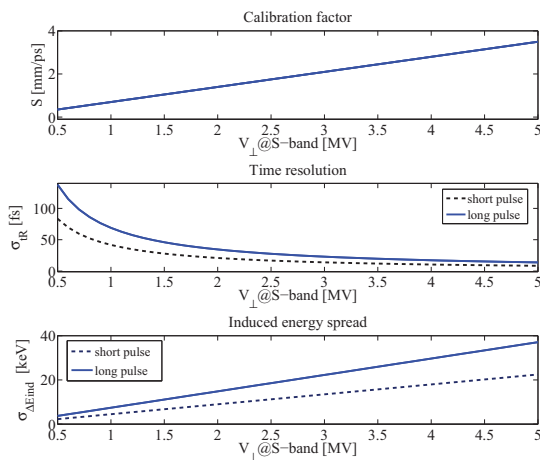


Figure 3: TDS-1 calibration factor, time resolution and induced energy spread as a function of the integrated deflecting voltage for short and long pulse options.

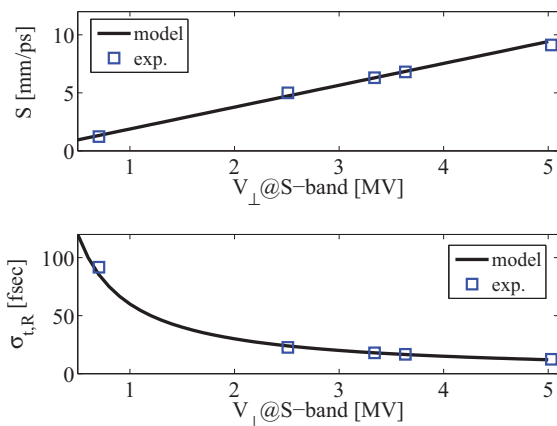


Figure 4: Calibration factor (up) and time resolution (bottom) as a function of integrated deflecting voltage. $E = 200 MeV$, $\beta_s = 10m$, $\beta_d = 40m$, $\varepsilon_{N,y} = 0.5 \mu rad$.

higher giving a factor 4 improvement from eq. 2. In addition, the higher kick per meter can also be achieved at higher frequency. Table 3 lists RF parameters for C-band and X-band deflecting structures presently in operation in

ISBN 978-3-95450-126-7

the FELs SACLA [6] and LCLS [7, 8]. Furthermore in the table there are also RF parameters for the X-band deflecting structure developed at Radiabeam Technologies [9].

Figure 5 shows the TDS-2 calibration factor, time resolution and induced energy spread as a function of the integrated deflecting voltage for short pulses, long pulses and high resolution options. Time resolutions are approximately 2.6 fs rms and 1.7 fs rms for the long and short pulse options in the nominal condition at 70 MV. Such time resolutions permit one to resolve the long pulse beam profile with approximately 10 slices but they are not enough to resolve the short pulse option. Using the high resolution option in table 1 then the rms time resolution improves to approximately 0.66 fs at 70 MV and such a resolution can resolve 3-4 slices in the beam profile. Induced energy spreads from the TDS-2 are below 300 and 200 keV rms for long and short options, respectively while it is approximately 500 keV rms with the high resolution option at 70 MV. The longitudinal phase-space will be measured at the screen centered in the Aramis energy collimator before the undulator chain. The dispersion is 0.115 m and the function can be reduced to 1 m in order to improve the energy resolution of the spectrometer to about 300 keV for the worse case that is the long pulse option at 5.8 GeV. It is worthwhile noting that induced energy spreads are on the order of magnitude of the spectrometer resolution in the energy collimator. Figure 6 shows the TDS-2 calibration factor, time resolution and induced energy spread as a function of the integrated deflecting voltage at X-band frequency for the long pulse and high resolution options. Time resolutions are approximately 1.9 fs rms and 0.48 fs rms for the long and high resolution options at 48 MV. Such time resolutions do not permit really larger improvements of the resolution obtained at C-band frequency. In this case the rms induced energy spreads are approximately 400 and 650 keV for long and high resolution options, respectively. The main electron linear accelerators in the Swiss FEL will use a 5.712 GHz C-band RF system and the last C-band module of the linac 3 will share the RF power source with the TDS-2 system. The available RF power from the S30CB13 klystron is 50 MW with maximum pulse duration of $3.5 \mu s$ and a repetition rate of 100 Hz. Furthermore a Barrel Open Cavity (BOC) pulse compressor will be used to increase RF power for the TDS as in the standard RF module [10]. In

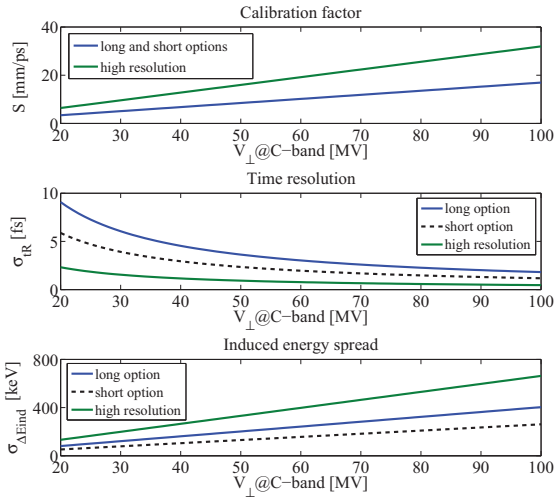


Figure 5: TDS-2 calibration factor, time resolution and induced energy spread as a function of the integrated deflecting voltage at C-band frequency for short pulses, long pulse and high resolution options.

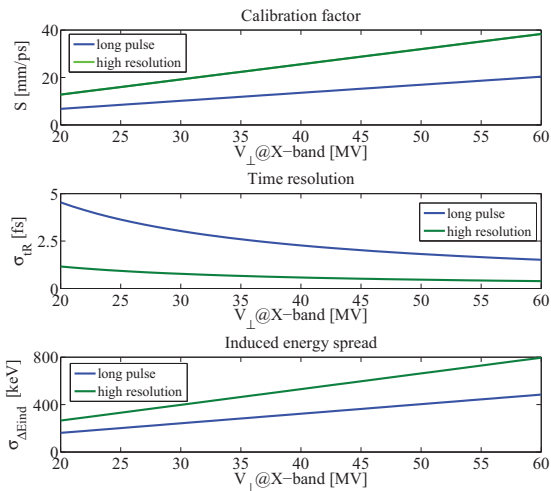


Figure 6: TDS-2 calibration factor, time resolution and induced energy spread as a function of the integrated deflecting voltage at X-band frequency for long pulse and high resolution options.

this way a deflecting voltage of 70 MV could be achieved with a set of two TDS of table3. Figure 7 shows a sketch of the C-band TDS power distribution. A critical component of this system is the RF switch since it will be under vacuum and at high C-band RF power. Furthermore another shutter switch will be likely needed to effectively switch off the TDS during the normal operation of the linac.

Effects of the Tuning Errors at Higher Voltage

In order to estimate effects of the RF tuning errors of the TDS a number of configurations having randomly cell-to-cell phase advance errors were used to estimate several

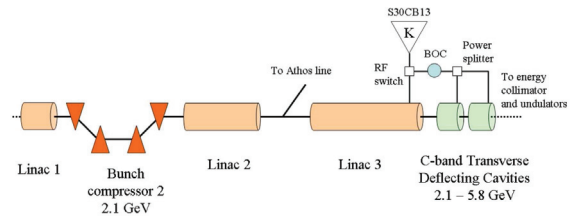


Figure 7: C-band TDS-2 power feeding scheme.

trajectories in the deflector itself. Figure 8 shows the effect of the tuning errors for 200 random configurations on the transverse displacement of the centroid (up) and on the angular divergence (bottom) as a function of the longitudinal coordinate inside one deflector. The beam energy is 2.1 GeV and integrated deflecting voltage 35 MV at C-band frequency. We considered a normal distribution of the errors along the deflector with mean zero and standard deviation of 1 deg. Besides in each cell an integrated phase error is considered. The beam offset is 1.2 mm rms while the angular divergence is 1.6 mrad at the deflector output. In

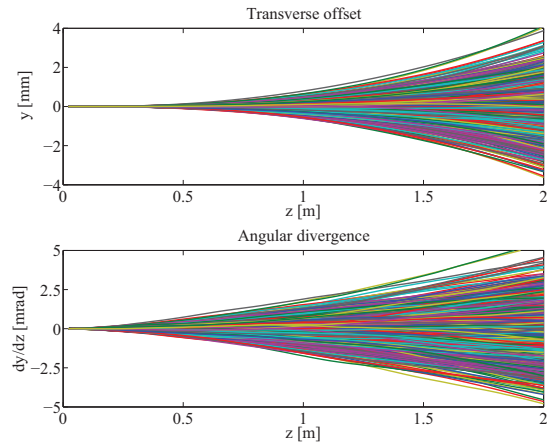


Figure 8: Effects of the tuning errors on the transverse displacement of the centroid (up) and on the transverse kick (bottom) as a function of the longitudinal coordinate inside one TDS-2.

order to limit these values of the beam offset and angular divergence at the deflector output we only chose error distributions with an integrated phase error along the structure lower than 5 deg. Figure 9 shows 41 error distributions that have an integrated phase errors less than 5 deg. Figure 10 shows the effect of these 41 error distributions on the transverse displacement of the centroid (up) and on the transverse kick (bottom) as a function of the longitudinal coordinate inside one TDS. In this case the beam offset is 0.26 mm rms while the angular divergence is 0.23 mrad at the deflector output. Effects of the tuning errors on the transverse displacement and angular divergence could be quite big if a limit on the integrated phase error is not properly fixed. Residual effects of the tuning error on the phase advance can still be compensated by adjusting globally the RF phase of the TDS-2 system. Then only an offset would

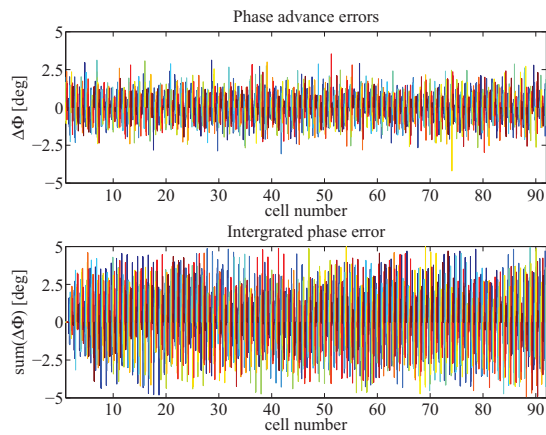


Figure 9: 41 seeds with integrated phase errors less than 5 deg.

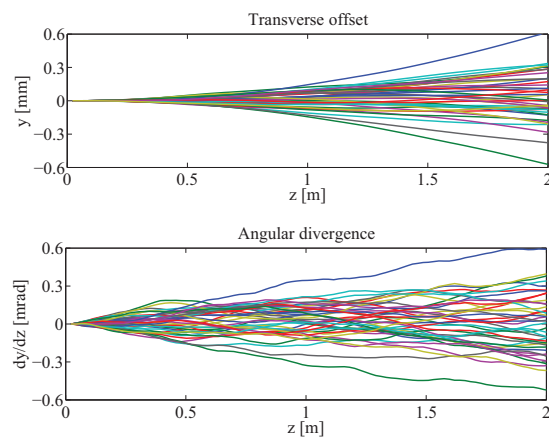


Figure 10: Effects of the tuning errors on the transverse displacement of the centroid (up) and on the transverse kick (bottom) as a function of the longitudinal coordinate inside one TDS-2.

remain, which should not be a severe problem for the measurements.

Effects of the RF Phase and Arrival Time Jitters at Higher Deflecting Voltage

In order to estimate effects of the RF phase jitter σ_ϕ at higher deflecting voltage we considered the motion of the beam centroid on the screen at the zero-crossing:

$$\sigma_{\langle y \rangle} \approx \frac{eV_\perp}{pc} \sqrt{\beta_d \beta_s} \sin \Delta\psi \sigma_\phi \quad (4)$$

and compared it with streaked beam at the screen $\sigma_y = S\sigma_z$. Considering the estimated RF phase jitter of 0.036° C-band [1] and a deflecting voltage V_\perp of 70 MV then for the long and short pulse options expected jitter of the streaked beam is approximately $200\mu m$ (rms) that is in the same order of magnitude of the beam size of the streak beam on the screen for the long pulse ($\sigma_y = 300\mu m$) while is a factor 8 higher than the streaked beam size on the screen for the short pulse ($\sigma_y = 24\mu m$). For the high res-

olution option the centroid jitter is approximately $400\mu m$ rms that is a factor 9 higher than the streaked beam size on the screen ($\sigma_y = 44\mu m$).

The arrival-time jitter translates to a transverse position jitter of the streaked beam through the calibration factor S , which is 12 and 22 mm/ps for long pulse and high resolution options at 70 MV, respectively. The expected arrival time jitter for the SwissFEL is 9 fs rms [1] and this value corresponds to $100\mu m$ and $200\mu m$ rms in the long pulse and high resolution options, respectively. The latter case produces a streaked beam jitter on the screen a factor 4.5 higher than the transverse size of the streaked beam. With reference to the field of view of the screen of 6 mm (horizontal) x 15 mm (vertical), the centroid jitter of the streaked beam seems to be acceptable and can tolerate arrival time jitter even up to 100 fs rms. Furthermore the maximum RF phase jitter at the zero-crossing phase that can be tolerated by the vertical screen size is about 0.1° C-band rms. Along the 5.8 GeV linac, 23 betatron collimators with variable vertical gaps are foreseen as well as a magnetic energy collimator just upstream the undulator beam line. For a larger variation of the TDS-2 RF phase, the energy collimator should provide the required protection to the machine and in particular to the undulator chain. On the other hand with the TDS-2 located at the high energy end of the main linac and with the betatron collimators mostly upstream of TDS-2, it is not still clear if the undulators are sufficiently protected against an unexpected RF phase shift of the deflecting structures. Since such unexpected phase shifts are almost impossible to exclude, finally dedicated collimators for TDS-2 operation need to still be considered.

Screen and Camera System Resolution

The resolution of the transverse profile monitor of $10\mu m$ is sufficient to resolve the un-streaked beam size which will be $20\mu m$ rms for the short pulses option of $10pC$.

CONCLUSION

In this paper we presented the TDS-1 and TDS-2 measurement systems to be used at SwissFEL, with a particular emphasis on the high energy transverse deflecting structures located at the linac-end. We verified that actual deflector structure used in the SITF satisfies specifications for TDS-1 system of the SwissFEL. In addition, time resolution was also verified by means of a campaign of measurements and it appears to be approximately 12.4 fs at 5 MV. The main electron linear accelerators in Swiss FEL will use a 5.712 GHz C-band RF system and the last C-band module of the linac 3 will share the RF power source with the TDS-2 system since the required deflecting voltage of 70 MV can be achieved with a set of two TDS at C-band frequency. On the other hand the present LCLS X-band deflector with one 50 MW X-band klystron does not permit really larger improvements of the resolution obtained at C-band frequency. Effects of the tuning errors on the transverse displacement and angular divergence were analyzed. As a conclusion they could be significant if a limit

on the integrated phase error is not properly fixed. Finally the effects of the RF phase and arrival time jitters at higher deflecting voltage were also taken into account. In this case the most important issue could come from unexpected RF phase shifts that are almost impossible to exclude and thus dedicated collimators for TDS-2 operation should be considered.

ACKNOWLEDGMENT

We would like to thank R. Zennaro (PSI) for useful discussion about the RF structures and power feeding scheme.

REFERENCES

- [1] R. Ganter et al., SwissFEL CDR, PSI Bericht Nr. 10-04, April 2012.
- [2] P. Emma, J. Frisch, P. Krejcik, "A transverse RF deflecting structure for bunch length and phase diagnostic", Proceedings of PAC 2001, Chicago, USA, 2001.
- [3] C. Behrens and C. Gerth, Proceedings of DIPAC09, Basel, Switzerland, 2009.
- [4] D. Alesini et al., Nuclear Instruments and Methods in Physics Research A 568 (2006) 488-502.
- [5] T. Schietinger et al., Proceedings of IPAC 2012, New Orleans, Louisiana, USA, 2012.
- [6] H. Ego et al., Proceedings of PAC 2011, San Sebastián, Spain, 2011.
- [7] Y. Ding et al., "Femtosecond x-ray pulse temporal characterization in free-electron lasers using a transverse deflector", PR STAB 14, 120701 (2011).
- [8] J. Wang and S. Tantawi, Proceedings of LINAC 08, Victoria, BC, Canada, 2008.
- [9] L. Faillace et al., Proceedings of PAC 2010, Kyoto, Japan, 2010.
- [10] F. Loehl et al., "Status of the SwissFEL C-band linear accelerator", these proceedings.